

## Photoelastic Visualization of Residual Stresses in PLA After Interlayer Shot Peening During Fused Filament Fabrication

Christian Sosa<sup>1</sup>, Lila Johnson<sup>1</sup>, Melanie Charron<sup>1</sup>, Noah Brinker<sup>1</sup>, Noah Stenberg<sup>1</sup>, Elena Parial<sup>1</sup>,  
Langdon Feltner<sup>2</sup>, Paul Mort<sup>2</sup>, Michael P. Sealy<sup>1\*</sup>

<sup>1</sup> School of Mechanical Engineering, Purdue University, West Lafayette, IN 47907, U.S.A.

<sup>2</sup> School of Materials Engineering, Purdue University, West Lafayette, IN 47907, U.S.A.

### Abstract

The ability to map high resolution residual stress fields from hybrid additive manufacturing is challenging. In this study, a hybrid method combining fused filament fabrication (FFF) with interlayer shot peening was employed in transparent polylactic acid (PLA) to visualize compressive residual stress fields. Residual stress is influenced both by the thermal conditions during layer deposition and the mechanical effects of shot peening. Specifically, understanding the influence of interchanging printing and peened layers on the internal stress distribution in polymers remains largely unexplored. This study addresses that gap by applying photoelastic stress analysis to visualize and compare birefringence patterns in PLA with multiple peened layers. Analyzing changes in birefringent intensity and distribution provides insight into how process modifications affect internal stress development. These findings highlight the potential of interlayer shot peening to tailor residual stress profiles and enhance the performance and reliability of polymer-based AM components.

*Keywords:* hybrid additive manufacturing, shot peening, photoelastic analysis, residual stress, birefringence

### 1. Introduction

Additive manufacturing, or 3D printing, is revolutionizing the design and manufacturing of components within industries. By printing components layer-by-layer from digital representations, AM facilitates quick prototyping and intricate geometries that cannot be achieved with conventional techniques. Of the various AM methods, fused filament fabrication is widely applied to the manufacturing of components made of thermoplastics because it is accessible and economical. It is a technique that extrudes molten thermoplastics from a nozzle to build a component layer by layer. FFF-printed components are, however, prone to internal residual stresses caused by non-uniform cooling and thermal gradients, which degrade mechanical performance, accuracy of dimensions, and long-term endurance.

Controlling the internal residual stress of polymer-based parts is an important challenge to making reliable 3D-printed components. To counteract such challenges, hybrid additive manufacturing techniques have been developed, incorporating secondary treatment during the build to enhance part properties. One of the promising techniques is interlayer shot peening—a

mechanical treatment that introduces compressive residual stresses by impacting surfaces with high-speed media. As shot peening has been demonstrated to be effective in optimizing mechanical performance in polymer components after fabrication, there is scant knowledge of the influence of in-situ interlayer shot peening has on internal stress development during the process itself of FFF.

Literature to date has tended to concentrate on surface-level modifications or tensile test results, not always supported by direct visualization of internal stress distributions. This is even more notable specifically in polymer-based AM components, where optical transparency provides great potential for stress field visualization. The goal of this study is to compare and visualize internal residual stress distributions in transparent PLA FFF-printed specimens experiencing different levels of shot peening interlayers. Using photoelastic characterization under polarized light, we qualitatively and quantitatively evaluate how frequency of peening affects the intensity and distribution of stress. From the results, we gain insight into how internal stress profiles in hybrid AM systems can be tailored using interlayer treatment with implications for enhancing the structural performance and reliability in polymer components.

## 2. Literature Review

Understanding stress distribution within components is essential when optimizing their mechanical properties. Residual stresses within printed and traditionally wrought parts are a critical issue when understanding the performance of parts, particularly in FFF (fused filament fabrication), due to the uneven thermal gradients and cooling cycles during the layer-by-layer deposition. Understanding and controlling these internal stresses continues to be a major challenge and there is a large gap in understanding the effects that hybrid techniques have in AM produced parts, especially in polymer systems like PLA.

Interlayer shot peening is a manufacturing method that provides a potential solution to controlling residual stresses within a part by inducing controlled compressive stresses upon layers during the printing process. Studies have demonstrated in FFF printing of ABS that periodic peening has altered the stressed distributions within the printed part. In the case of Hadidi et al. (2019), their research found that peening the parts every four to five layers enhanced the energy absorption within the part, while excessive peening had weakened the part, making it more brittle [1]. This study highlights that more research needs to be done to understand the interlayer peening process to create a more balanced method. Similarly, Herianto et al. (2023) showed that only peening the outer surface increased the tensile strength in PLA FFF printing [2]. The findings in both studies have provided insight to how shot peening in polymers can effectively increase the strength of the parts as well as modify the stress. Neither of these studies directly visualize the internal stress fields of the samples to understand what is happening to the stress distributions within the parts, which is a critical component to be addressed by our work.

The pattern and the spacing of peening have been proven to significantly influence stress outcomes within all peened parts. Over peening and under peening samples can plastically deform the sample reducing the strength or not induce enough residual stresses to have a meaningful effect on the part performance. Xiao et al. (2018) compared random and regular peening on samples and found that the regular patterns produced more uniform compressed stress fields, while the random

peening had resulted in more localized tensile stress and variability [3]. Although peening of individual layers introduces variation, our study uses regular interlayer spacing between peened and not peened layers to create as structured internal stress fields as possible.

Denise (2023) applied LSP (laser applied laser shock peening) during FFF of PLA and found that both energy and regularity of the input were crucial in shaping interlayer bonding stress and evolution [4]. Though LSP uses a different mechanism topeen the samples vs. mechanical shot peening, the effects of the induced compressive stresses are comparable. Denise's findings continue to reinforce our hypothesis that interlayer treatments can tailor stress fields and help to improve the mechanical integrity of the samples. The findings in our study will help to build on these results by transitioning from the inferred machinal improvements by means of tensile testing to directly observe the stress patterns.

Photoelastic analysis is a valuable qualitative process as it can visualize internal stress fields in transparent, birefringent materials. Under polarized light, the internal stresses manifest as interference fringe patterns, allowing for the stress magnitude and concentration points to be qualitatively and quantitatively assessed. Orr and Finaly (1997) provide a foundational theory which explains how birefringent fringes correlate with stress gradients [5]. Ueda et al. (2004) demonstrate different conditions that samples are subjected to influence their internal stresses and allow for comparative evaluation in dental implants under load [6]. Stress distributions appearing as birefringence are observable using a polariscope coupled with material that allows light to pass through [6]. By using interlayer shot peening on transparent PLA and a polarized light setup, this research aims to visualize internal stress fields not only caused by external forces but those affected by the fabrication process itself. In polymers, Scafidi et al. (2015) recommend RGB photo elastically and phase shafting for more precise, quantitative stress mapping methods that are adaptable to our ImageJ based hue and threshold for individual segmentation analysis [7].

Despite the known effects of peening, both mechanically and through LSP methods, no studies have used the technique of photoelasticity to integrate the combination of peening and visual analysis to create a clear picture of the internal residual stress fields in hybrid AM processes. Current research infers stress through mechanical testing or simulations, while our work addresses the gap in this methodology by applying photoelastic analysis to systematically varied interlayer peening conditions. Offering a visual and measurable framework for understanding stress evolution in polymer parts via transparent PLA, our approach enables direct observation of how interlayer treatments influence internal stress distributions, providing a novel experimental basis for optimizing hybrid AM designs and validating stress control strategies.

### **3. Experimental Procedure**

#### **3.1 Fused Filament Fabrication (FFF)**

This research examined how interlayer shot peening influences residual stresses in PLA parts fabricated using fused filament fabrication (FFF). In the FFF process, molten thermoplastic is extruded through a heated nozzle to build parts layer by layer (**Fig. 1**).

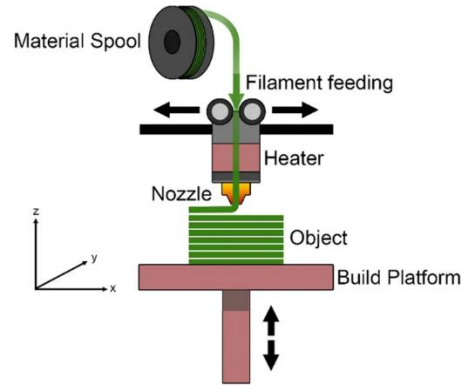


Fig 1. Illustrative diagram of FFF process.

All specimens were printed using transparent PLA on a Luzbolt Mini FFF 3D printer (Fig. 2). The sample geometry followed standardized Almen strip specifications suitable for residual stress studies (Fig. 3). The printing parameters used in this study are listed in Table 1.

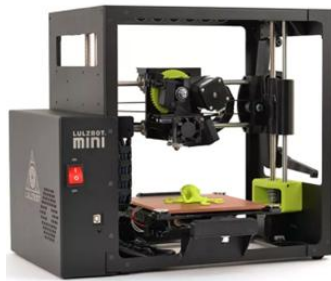


Fig 2. Luzbolt mini FFF 3D printer.



Fig 3. Almen strips used to measure peening intensity.

Table 1. FFF process parameters for specimen fabrication

Parameter	Value
Filament Material	Transparent PLA
Filament Diameter	1.75 mm
Layer Height	0.20 mm
Nozzle Diameter	0.40 mm
Line Width	0.60 mm
Print Speed	30 mm/s
Nozzle Temperature	210°C
Bed Temperature	60°C
Infill Density	100%
No. of Layers	10
Printing orientation	Alternating 0°/90° (every layer)
Sample Dimensions	76.6 × 19.05 × 2.00 mm

### 3.2 Shot Peening

Interlayer shot peening was employed to investigate its effect on residual stress development in 3D-printed PLA parts. Shot peening introduced compressive residual stresses by bombarding the surface with high-velocity media.

A total of twelve samples were divided into four groups: one control (no peening) and four treatment groups with 2, 3, 4, or 5 peened layers. During fabrication, after each target layer was completed, the build plate was removed from the 3D printer, transferred to the shot peening system for treatment, and then returned to the printer to resume printing. This process was repeated for each peened layer, following the configurations shown in **Fig. 4**. Shot peening was performed using a compressed-air system with a fixed nozzle-oriented perpendicular to the sample surface. The build platform moved laterally under the nozzle to ensure uniform coverage (**Fig. 5 and Fig. 6**).

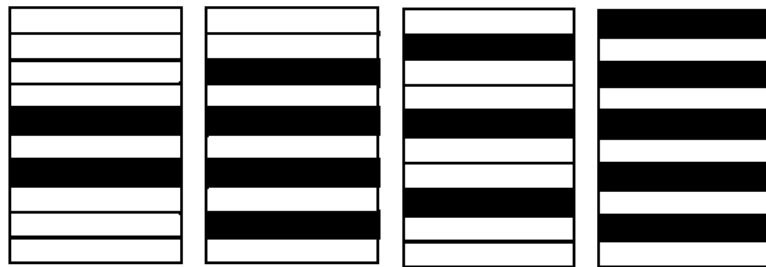


Fig 4. Schematic representation of peened (black) vs. unpeened (white) layers.



Fig. 5. Shot peening system used for interlayer treatment.

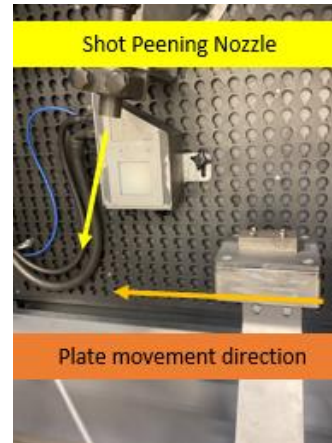


Fig. 6. Shot peening nozzle orientation and plate movement direction.

Peening was performed using a fixed nozzle positioned perpendicular to the sample surface. The nozzle was traversed laterally during each pass to ensure uniform coverage. Process parameters are detailed in Table 2. An example of a completed specimen with three peened layers is shown in **Fig. 7**.

Table 2. Shot peening process parameters used during interlayer treatment of PLA specimens

Parameter	Value
Air Pressure	2.0 bar
Media Flow Rate	3.0 kg/min
Coverage	100% (single pass)
Peening Method	Interlayer (during printing)
Peened Layers	3, 4, or 5 (depending on group)
Nozzle Orientation	Perpendicular to part surface
Peening Symmetry	Symmetrical about mid-plane

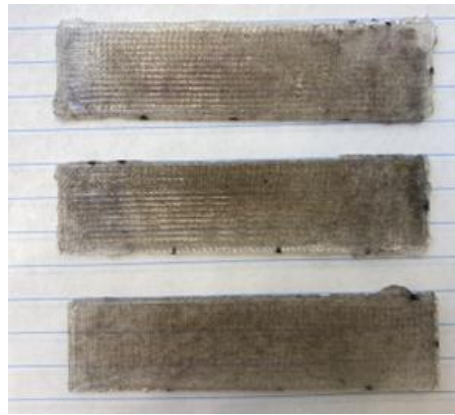


Fig. 7. Example of samples with 3 peened layers.

### 3.3 Sample Characterization

In order to visualize the stress fields under the microscope, each of the printed samples needed to be compressed to a specific degree such that the same amount of bending stress ( $\sigma$ ) was uniformly induced across each of the samples. To do this, each of the sample's geometry needed to be characterized by calculating the required bending displacement to induce an equivalent stresses state, while ensuring that the stress remained within the elastic region of the material.

To achieve consistent applied stress across each of the samples with slightly varying geometries, a reference sample was compressed by 2 mm, and the resulting stress was calculated. This provided a baseline bending stress ( $\sigma$ ), which was then used to determine the required compression and curvature needed for each of the other samples. The bending stress (MPa) in a beam under pure bending conditions is given by  $My/I$ , where  $M$  is the bending moment (Nm),  $y$  is the perpendicular distance from the neutral axis (m), and  $I$  is the second moment of inertia ( $m^4$ ). The bending stress is assumed to remain in the linear elastic region and shear deformation is negligible. The bending moment is given by

$$M = \frac{EI}{\rho_n}$$

where  $E$  is the Young's modulus or elastic modulus ( $\frac{N}{m^2}$ ), and  $\rho$  is the corresponding radius of curvature ( $m$ ). The expression for finding the perpendicular distance from the neutral axis ( $y$ ) is  $t_n/2$ , where  $t_n$  is the thickness of the sample. The second moment of inertia ( $I$ ) is given by  $\frac{w_n t_n^3}{12}$ , where  $w_n$  is the width of each of the samples. By combining each of these expressions and simplifying, the bending stress equation can be expressed as:

$$\sigma = \frac{E y}{\rho} \rightarrow \frac{E y_1}{\rho_1} = \frac{E y_2}{\rho_2}$$

Since all the material and elastic modulus,  $E$ , are assumed to be constant across each of the equivalent samples, the stress equivalence condition is reduced to:

$$\frac{y_1}{\rho_1} = \frac{y_2}{\rho_2}$$

From the geometry of a circular arc, the relationship between the arc length of each of the samples and the radius of curvature is defined as:

$$L_n = \rho_n \cdot 2 \sin^{-1} \left( \frac{\theta_n}{2} \right) \text{ and } L_n^* = \rho_n \cdot 2 \sin^{-1} \left( \frac{L_n}{2\rho_n} \right)$$

This provides the key relationships between the unbent length of a sample,  $L_n$  (m), and the new bent length of a sample,  $L_n^*$  (m). This relationship relies on the radius of curvature of the sample,  $\rho_n$ , and the central angle,  $\theta_n$  (rads).

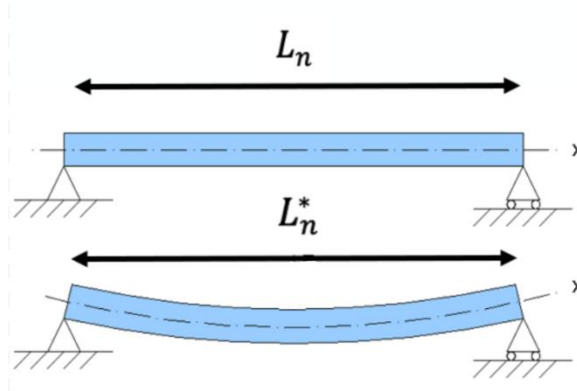


Fig. 8. Bent vs. unbent sample lengths.

**Fig. 8** visualizes the difference between the compressed and original samples. Given that the initial reference sample was compressed by 2mm, its new bent length results in  $L_n^* = L_1 - 0.002(m)$ . Using the reduced length, the corresponding radius of curvature,  $\rho_1$ , was calculated. This value was then used to find the required  $\rho_2$  for the next sample to maintain the same stress. Once  $\rho_n$  was known, the required compressed length  $L_n^*$  for each sample could be found using the inverse of the arc length formula, ensuring that  $\sigma_1 = \sigma_2$ .

The experimental steps can be summarized as follows: each sample's dimensions were measured (width  $w_n$ , thickness  $t_n$ , and original length  $L_n$ ) for each printed sample. Using the calculations listed, the stress generated by compressing the reference sample was calculated. By holding the stress constant and calculating the appropriate radius of curvature, each of the sample's new bent length,  $L_n^*$ , was determined. Finally, each sample is ready to be bent to its calculated compressed length prior to being placed under microscope for stress field imaging.

### 3.4 Photoelastic Analysis

To visualize internal stress distribution, samples were analyzed using photoelastic techniques. Arieneplast transparent PLA was selected specifically to enable light transmission under polarized conditions, allowing stress-induced birefringence patterns to be observed and recorded. Birefringence occurs when light passes through anisotropic materials, such as stressed polymers, causing it to split into two beams due to varying refractive indices. This phenomenon produces phase retardation, which appears as visible color shifts or intensity variations under polarized light. These changes provide insight into internal stress distributions and material defects. Polarized lenses placed above and below the sample enhance these patterns by filtering the light directionally (**Fig. 9**).

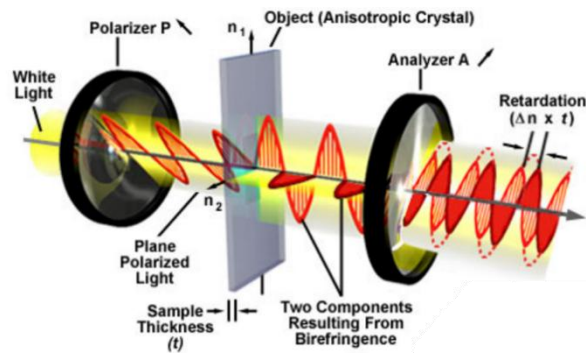


Fig. 9. Birefringent crystals between crossed polarizers [8].

Photoelastic evaluation was conducted using an Olympus BX-51 fluorescence optical microscope (**Fig. 10**). It is equipped with polarized lenses located above and below the specimen stage (**Fig. 11**). A  $2\times$  magnification lens was used to capture a broad field of view suitable for comparing stress patterns across the sample surface. The polarized lenses filter the light passing through the sample, revealing regions of internal stress through variations in light interference and color intensity.



Fig. 10. Olympus fluorescence optical microscope used for polarized light.

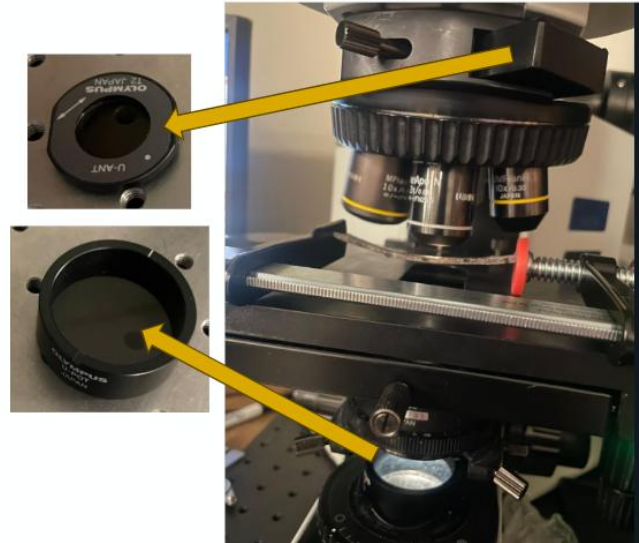


Fig. 11. Polarized lenses used to measure birefringence.

A compressive load was applied to the samples during observation. Using digital calipers, each specimen was clamped to a set compressed length prior to imaging. Three loading conditions were examined:

1. Compression to a calculated uniform-stress length
2. Compression near the material's failure point
3. Compression to an intermediate length (average of the two)

The load was applied using a manual clamp setup (Fig. 12). Each sample was imaged under the microscope at three locations: both ends and the center (Fig. 13). The resulting birefringent patterns were recorded using the microscope's camera system and later processed for comparison.

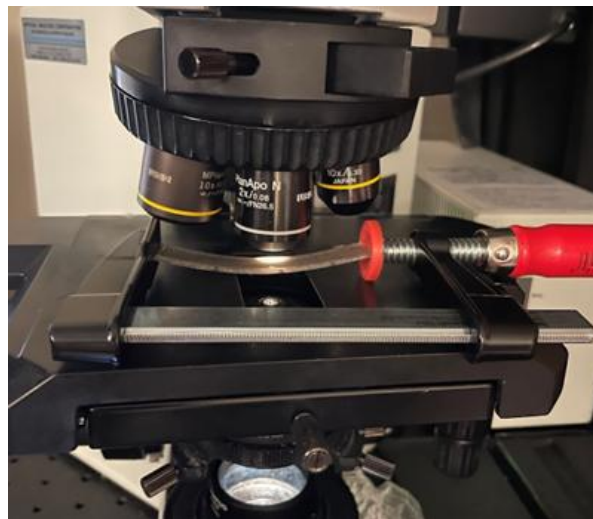


Fig. 12. Compressive load set up.

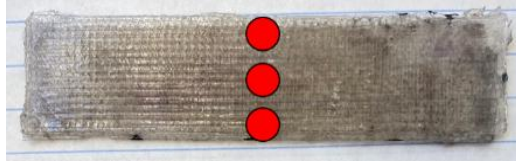


Fig. 13. Locations of observation on each sample.

Captured birefringence images were processed using ImageJ (NIH, U.S.) to extract both the magnitude and spatial distribution of internal stresses. Each experimental condition (control, 2, 3, 4, and 5 peened layers) included 9 images (top, middle, and bottom for each of three samples), totaling 54 images. Two complementary image analysis methods described below were employed.

### 3.4.1 Method 1: Hue-Based Stress Magnitude Analysis

Each image was converted to a Hue Saturation Brightness (HSB) stack. The first slice, corresponding to the hue channel, was used to assess relative stress magnitude, as hue reflects the purity of color produced by birefringence. The “Analyze” and “Measure” functions were used to extract the mean, maximum, and standard deviation of hue intensity. Histograms were also generated and exported for comparative evaluation across samples. **Fig. 14** shows both the original polarized image and the corresponding hue channel used in this analysis.

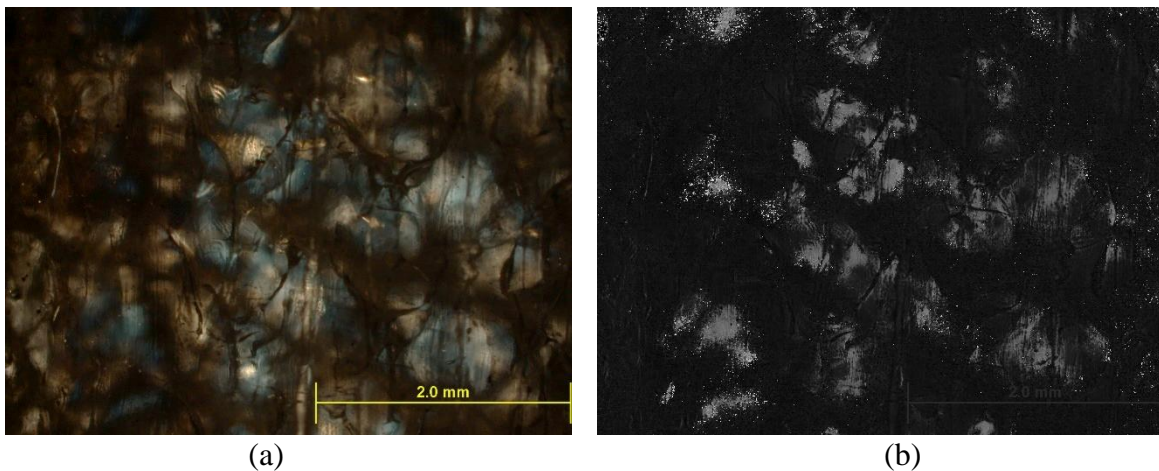


Fig. 14. Five-layers peened (a) Original polarized image (b) Corresponding hue channel from HSB stack used for stress magnitude analysis.

### 3.4.2 Method 2: Area-Based Threshold Segmentation

To quantify the percentage of the sample under stress, each image was first converted to 8-bit grayscale. A fixed threshold value was then applied using the threshold tool to divide the image

into stress and non-stress regions (**Fig. 15**). This process produced a binary image where white pixels represented stressed areas, and black pixels represented the background. The complete transformation from the original polarized image to its binary form is illustrated in **Fig. 16**, and the percentage area under stress was calculated using pixel intensity histograms.

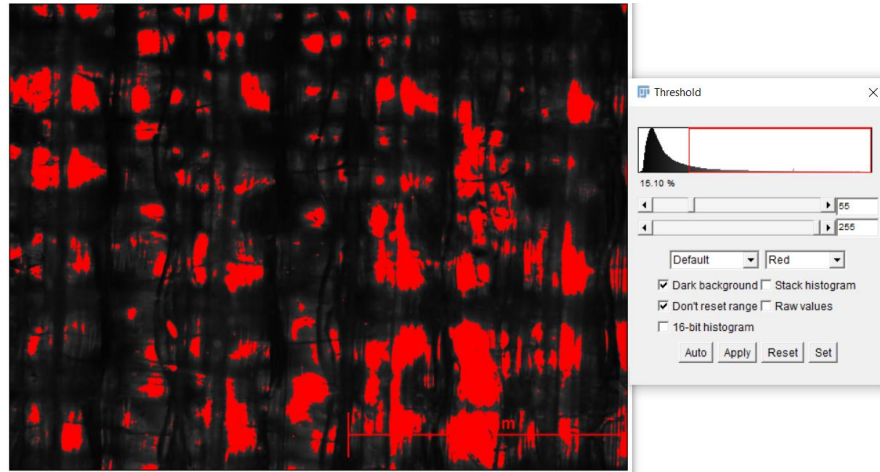


Fig. 15. Thresholding in ImageJ applied after 8-bit conversion to segment stress regions.

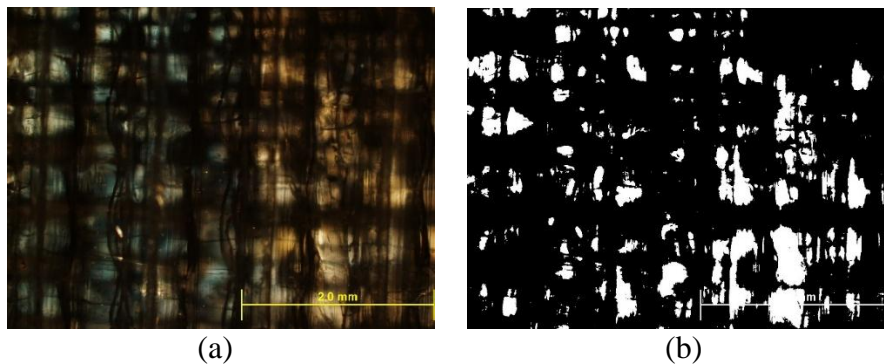


Fig. 16. Two layers peened middle with (a) polarized-light images (b) 8-bit with threshold.

## 4. Results

### 4.1 Stress Intensity and Location

Applying a compressive load to a calculated uniform-stress length (minimum load), to near the material's failure point (maximum load), and to an intermediate length were found to impact stress intensity and provide information about the location of stress. More saturated colors appeared in areas experiencing higher stress while duller colors indicated regions of lower stress. Highly concentrated color zones commonly appeared near the edges and were better observed in the middle of the sample when the compressed load increased. When the samples were compressed

to near failure, that is when the colors were most prominent and easiest to see since it allowed the most light to pass through. As shown in **Fig. 17**, the 5-layer peened sample was chosen due to it being the opaquet under the microscope, and the images for the middle section were selected since that is the location that showed the least stress. Therefore, the differences in loads were prominent enough to aid in obtaining qualitative information. In terms of stress intensity and location of stress, **Fig. 18** shows how different regions of the sample experiences varying levels of stress. The edges showed the most color while the middle was spottier.

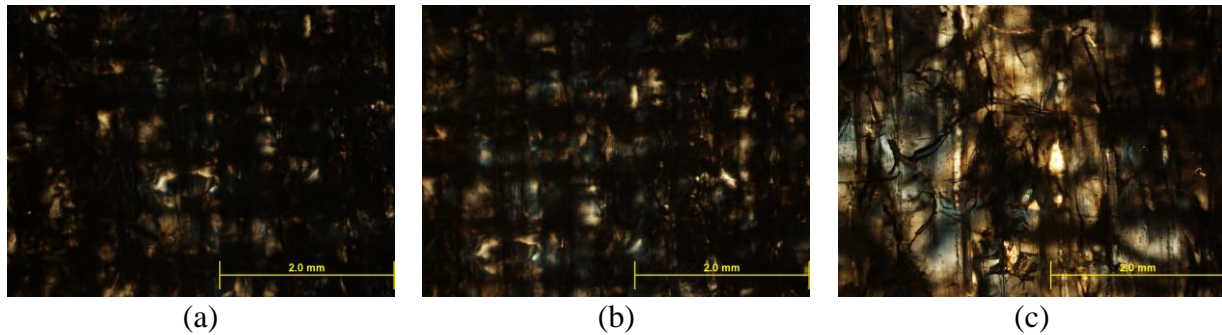


Fig. 17. Middle Section of a 5-layer peened sample while subjected to compression: (a) minimum load, (b) intermediate load, and (c) maximum load.

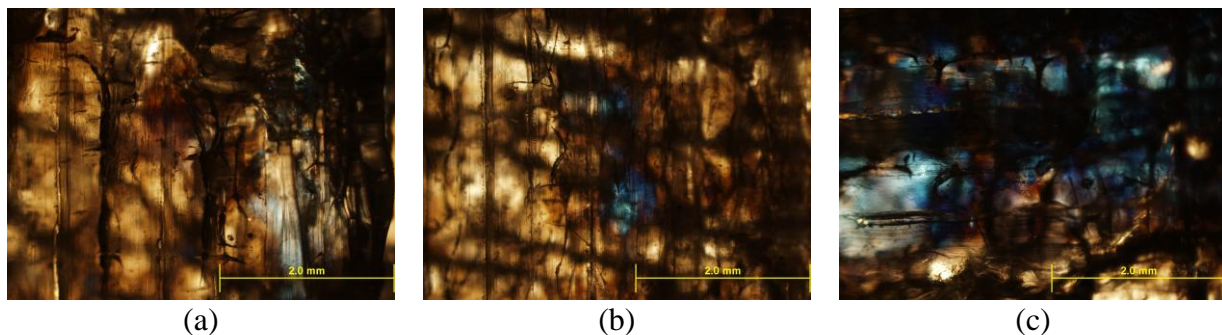


Fig. 18. Various locations of a 4-layer peened sample while subjected to its maximum load of compression: (a) left section, (b) middle section, and (c) right section.

## 4.2 Comparative Sample Evaluation

Multiple samples were tested under identical compressive loading conditions to evaluate how variations in peened layers affected stress visualization and distribution as well as the ability to use photoelastic analysis. Across the peening conditions, differences were observed in the intensity and clarity of the color fringes. For instance, the control sample without peened layers produced the most color and the most uniform distribution due to it being the most transparent. However, as shown in **Fig. 19**, the more layers peened, the sample becomes opaquer, limiting the amount of light passing through which reduces birefringence response.

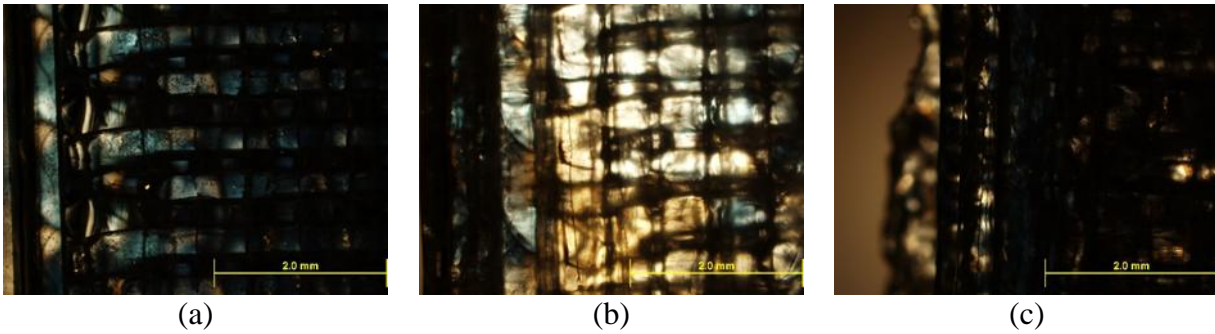


Fig. 19. Right Section of samples while compressed using the minimum load: (a) 0 layers peened, (b) 2 layers peened, and (c) 3 layers peened.

### 4.3 Mean Hue vs. Displacement Level

**Fig. 20** plots the mean hue for the control and for specimens with two, three, four, and five peened layers at three displacement levels (avg 1 is maximum, avg 2 is medium, avg 3 is minimum). Hue rises markedly in the control, climbing from about 33 to 52 units as displacement decreases. The same inverse trend appears in the peened samples but with smaller gains: roughly plus 4.9 units for two layers, plus 9.7 units for three layers, and plus 7.2 units for four layers. The five-layer sample behaves differently; its hue falls at the medium displacement and ends only about one unit above the starting value, suggesting optical masking from debris rather than a true stress response. All peened specimens begin at a lower baseline hue (approximately 21 to 27 units) than the control sample (about 33 units), indicating that shot peening alters the material's birefringence. Overall, additional peened layers progressively dampen and at five layers distort the hue response to displacement.

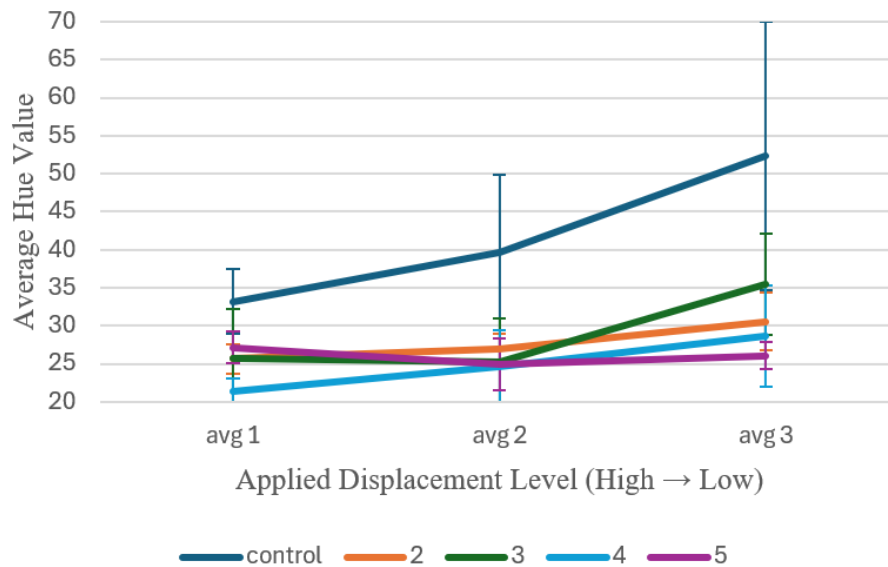


Fig. 20. Mean hue versus displacement.

#### 4.4 Visual Comparison at Successive Displacements

**Fig. 21** shows polarized-light micrographs taken from the left edge of the three-layer peened specimen at the maximum, medium, and minimum displacement settings. From image (a) to image (c) the central blue-green band becomes progressively darker and narrower, while the surrounding amber regions desaturate toward grey.

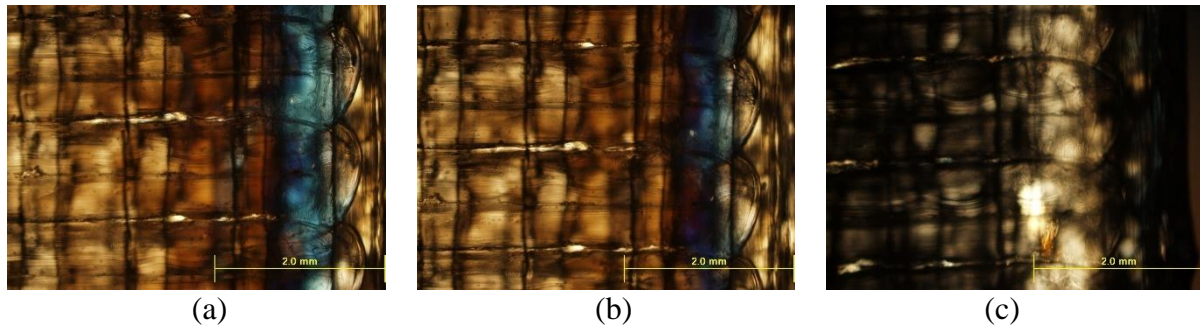


Fig. 21. Polarized-light images from the left side of the three-layer peened specimen at (a) maximum, (b) medium, and (c) minimum displacement.

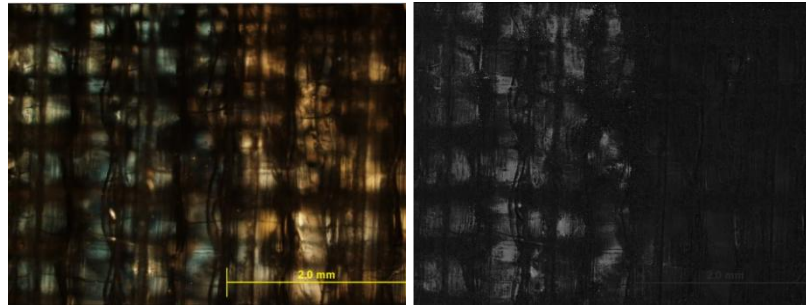
#### 4.5 Representative Output of Image Analysis

To illustrate the type of data obtained through the hue-based and threshold-based methods described in Sections 3.4.1 and 3.4.2, a representative example from the middle region of a 2-layer peened sample subjected to maximum displacement is presented in **Fig. 22** and **23**.

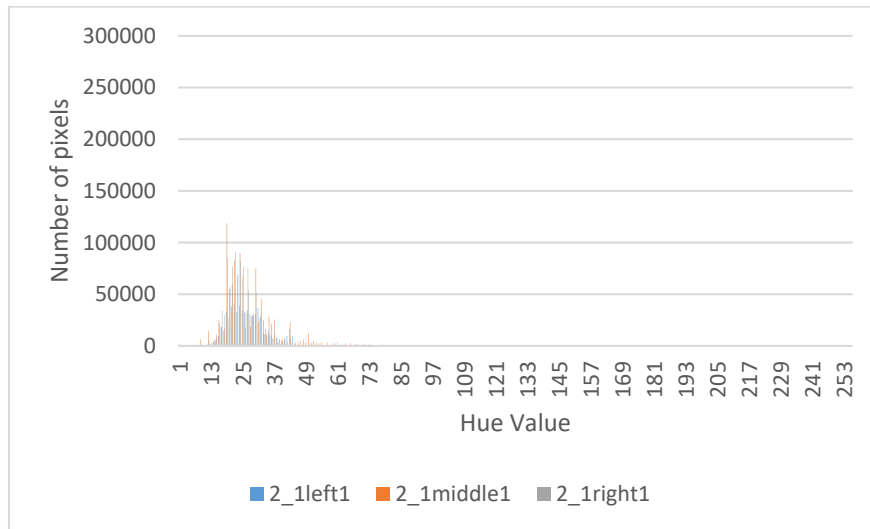
**Fig. 22a** shows the original polarized-light image alongside its corresponding hue map. The histogram in **Fig. 22b** displays the distribution of hue values per pixel, with a mean of 27.332 and a standard deviation of 13.113. The data reveal a predominance of low hue values, suggesting that most regions are under relatively low stress.

**Fig. 23a** presents the binary image of the same sample after threshold segmentation. The distribution of pixel intensities was converted into area percentages, indicating the proportion of the sample under stress. In the Table shown as **Fig. 23b** summarizes the threshold-based results, where 6.62% of the area was identified as stressed (white pixels), and 93.38% remained unstressed (black pixels).

Together, these outputs exemplify how both analysis methods capture different aspects of internal stress distribution: hue analysis provides information on stress intensity variation, while binary segmentation quantifies the spatial extent of stress across the sample.

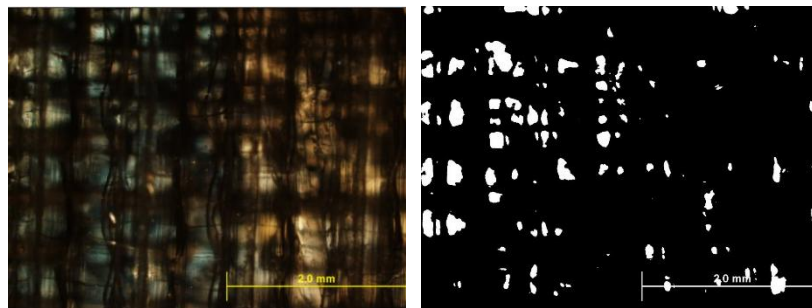


(a)



(b)

Fig. 22 (a) Polarized-light and hue-converted images of a 2-layer peened sample (middle region).  
 (b) Histogram showing the distribution of hue values per pixel.



Black Pixels (0)	White Pixels (255)	Black Area %	White Area %
1126940	79900	93.38%	6.62%

Fig. 23. (a) Polarized-light and binary image of the same sample after threshold segmentation.  
 The pixel counts and area percentage of stressed and unstressed regions are provided.

## 5. Discussion

### 5.1 Interpretation of the Results

When transparent PLA samples are observed under polarized light after shot peening, photoelastic analysis reveals internal stresses as color. These colors are caused by birefringence, and their intensity corresponds to the magnitude and distribution of internal stresses. For instance, more vibrant colors indicate areas of high stress while duller colors correspond to lower stress. With the stresses being most apparent near the sample's edges, similar to Ueda *et al.* (2004) and Orr and Finlay (1997), the location itself allows mapping of the color changes. By mapping the color changes, the maximum stress the part experiences can be visually identified and therefore predicted.

Using comparative sample analysis allows for identification of trends and differences in how the samples respond when under similar loading conditions. Similar to observations made by Hadidi *et al.* (2019) and Xia *et al.* (2018), our results show that peening interval and pattern significantly influence stress development. This comparison helped identify which peening conditions best revealed stress behavior under load. The ease of seeing colors depends on the number of peened layers, which provides insight into how many layers should be peened.

### 5.2 Limitations and Uncertainty Analysis

A notable limitation has to do with the photoelastic analysis of the 3-, 4-, and 5-layers peened samples. The shot peening process used steel beads, and the samples underwent 100% coverage, which is one pass over the component per layer peened. Qualitatively observed and shown in **Fig. 24**, the contamination from the beads impacts the transparency of the sample depending on the number of layers peened. Increasing the number of layers peened within a sample reduces the sample's overall transparency, ultimately causing impairment of light transmission during photoelastic analysis which hinders accurate visualization of internal stress patterns. For instance, **Fig. 25** shows a comparison of the reduced ability to observe color and stress uniformity due to the increase in number of layers peened. As a result, the reliability of the observed stress distributions decreases with increased peened layers. Cleaning the samples after each layer peened may reduce this limitation which can improve the clarity of results.



Fig. 24 Comparison of the contamination due to the number of layers peened.

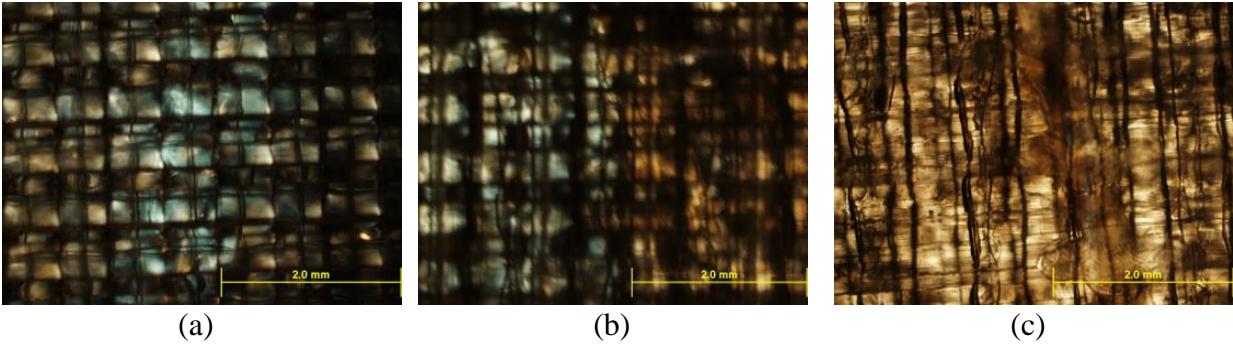


Fig. 25 Comparison of the ability to observe color and stress uniformity: (a) middle of 0 layers peened, (b) middle of 2 layers peened, and (c) middle of 3 layers peened.

## 6. Summary & Conclusions

This study examined the influence of interlayer shot peening on internal residual stresses in PLA components fabricated using fused filament fabrication. Shot peening was applied during selected layers of the printing process to introduce compressive stresses, and internal stress distributions were visualized using photoelastic microscopy under polarized light. Transparent PLA specimens with 0 (control), 2, 3, 4, and 5 peened layers were subjected to controlled bending, and stress patterns were analyzed using two digital image processing techniques: hue-based intensity analysis and threshold-based segmentation. The results demonstrated several key findings:

- Residual stress distributions within the printed PLA samples varied with the number of peened layers, as evidenced by differences in birefringence patterns.
- Increased compression produced more intense color fringes, confirming higher stress magnitudes.
- Observed differences in stress response across samples resulted from the interlayer peening configuration, independent of applied external load.
- While moderate peening improved stress modification, excessive peening led to opacity due to surface contamination, which diminished the effectiveness of photoelastic imaging.

These findings signify that photoelasticity is an effective, non-destructive method for visualizing residual stress inside components and for comparing effects of hybrid AM processes. By revealing how shot peening affects internal residual stress, the research contributes to safer and more reliable 3D-printed components. Ultimately, these findings could inform design rules and process improvements for next-generation additive manufacturing technologies making future devices safer, stronger, and more durable.

### Acknowledgements

The use of equipment and facilities was provided in part by the Manufacturing and Materials Research Laboratories (MMRL) at Purdue University. Also, we would like to acknowledge Prof. Paul Mort for access to shot peening equipment. Primary financial support was provided by NSF CMMI: 1846478 (rev. 2318705) titled, "CAREER: Hierarchical Structure

Integrity of Magnesium Alloys via Asynchronous Laser and Additive Processing” and the School of Mechanical Engineering at Purdue University.

### References

- [1] Hadidi, H., Mailand, B., Sundermann, T., Johnson, E., Madireddy, G., Negahban, M., & Sealy, M. (2019). Low velocity impact of ABS after shot peening predefined layers during additive manufacturing. *Procedia Manufacturing*, 34, 594–602. <https://doi.org/10.1016/j.promfg.2019.06.169>
- [2] Herianto, Mastriswadi, H., Nasution, A., & Atsani, S. (2023). Effect of Shot Peening Parameters on PLA Parts Manufactured with Fused Deposition Modeling. *Journal of Engineering & Technological Sciences*, 55(5), 513. <https://openurl.ebsco.com/EPDB%3Agcd%3A4%3A29573748>
- [3] Xiao, X., Tong, X., Gao, G., Zhao, R., Liu, Y., & Li, Y. (2018). Estimation of peening effects of random and regular peening patterns. *Journal of Materials Processing Technology*, 254, 13–24. <https://doi.org/10.1016/j.jmatprotec.2017.11.018>
- [4] Denise, F. (2023). Characterization of Interlayer Laser Shock Peening during Fused Filament Fabrication of Polylactic Acid (PLA). *Dissertations, Theses, and Student Research*. University of Nebraska–Lincoln. <https://digitalcommons.unl.edu/mechengdiss/195>
- [5] Orr, J.F., & Finlay, J.B. (1997). Photoelastic stress analysis. In *Optical measurement methods in biomechanics*. Springer. [https://doi.org/10.1007/978-0-585-35228-2\\_1](https://doi.org/10.1007/978-0-585-35228-2_1)
- [6] Ueda, C., Markarian, R. A., Sendyk, C. L., & Laganá, D. C. (2004). Photoelastic analysis of stress distribution on parallel and angled implants after installation of fixed prostheses. *Brazilian Oral Research*, 18(1), 45–52. <https://doi.org/10.1590/s1806-83242004000100009>
- [7] Scafidi, M., Pitarresi, G., Toscano, A., Petrucci, G., Alessi, S., & Ajovalasit, A. (2015). Review of photoelastic image analysis applied to structural birefringent materials: Glass and polymers. *Optical Engineering*, 54(8), 081206. <https://doi.org/10.1117/1.oe.54.8.081206>
- [8] Mortimer Abramowitz, Michael W. Davidson, Optical Birefringence, *Evident Scientific*, Accessed 06/2025. <https://evidentscientific.com/en/microscope-resource/knowledge-hub/lightandcolor/birefringence>